

## Basic Study

## Intercellular mitochondrial transfer as a means of revitalizing injured glomerular endothelial cells

Li-Xia Tang, Bing Wei, Lu-Yao Jiang, You-You Ying, Ke Li, Tian-Xi Chen, Ruo-Fei Huang, Miao-Jun Shi, Hang Xu

**Specialty type:** Cell and tissue engineering

**Provenance and peer review:**

Unsolicited article; Externally peer reviewed.

**Peer-review model:** Single blind

**Peer-review report's scientific quality classification**

Grade A (Excellent): A  
Grade B (Very good): 0  
Grade C (Good): C  
Grade D (Fair): 0  
Grade E (Poor): 0

**P-Reviewer:** Oliva J, United States; Prasetyo EP, Indonesia

**Received:** May 23, 2022

**Peer-review started:** May 23, 2022

**First decision:** July 6, 2022

**Revised:** July 18, 2022

**Accepted:** September 6, 2022

**Article in press:** September 6, 2022

**Published online:** September 26, 2022



**Li-Xia Tang, You-You Ying, Ke Li, Ruo-Fei Huang,** Department of Endocrinology, The First People's Hospital of Yongkang Affiliated to Hangzhou Medical College, Jinhua 321300, Zhejiang Province, China

**Bing Wei,** School of Medicine, Southeast University, Nanjing 210009, Jiangsu Province, China

**Lu-Yao Jiang,** Department of Medical Rehabilitation, The First People's Hospital of Yongkang Affiliated to Hangzhou Medical College, Jinhua 321300, Zhejiang Province, China

**Tian-Xi Chen, Miao-Jun Shi,** Department of Nephrology, The First People's Hospital of Yongkang Affiliated to Hangzhou Medical College, Jinhua 321300, Zhejiang Province, China

**Hang Xu,** Department of Hemodialysis/Nephrology, The First People's Hospital of Yongkang Affiliated to Hangzhou Medical College, Jinhua 321300, Zhejiang Province, China

**Corresponding author:** Hang Xu, BMed, Doctor, Occupational Physician, Department of Hemodialysis/Nephrology, The First People's Hospital of Yongkang Affiliated to Hangzhou Medical College, No. 599, Jinshan West Road, Dongcheng District, Jinhua 321300, Zhejiang Province, China. [13758989843@163.com](mailto:13758989843@163.com)

**Abstract****BACKGROUND**

Recent studies have demonstrated that mesenchymal stem cells (MSCs) can rescue injured target cells *via* mitochondrial transfer. However, it has not been fully understood how bone marrow-derived MSCs repair glomeruli in diabetic kidney disease (DKD).

**AIM**

To explore the mitochondrial transfer involved in the rescue of injured glomerular endothelial cells (GECs) by MSCs, both *in vitro* and *in vivo*.

**METHODS**

*In vitro* experiments were performed to investigate the effect of co-culture with MSCs on high glucose-induced GECs. The transfer of mitochondria was visualized using fluorescent microscopy. GECs were freshly sorted and ultimately tested for apoptosis, viability, mRNA expression by real-time reverse transcriptase-polymerase chain reaction, protein expression by western blot, and

mitochondrial function. Moreover, streptozotocin-induced DKD rats were infused with MSCs, and renal function and oxidative stress were detected with an automatic biochemical analyzer and related-detection kits after 2 wk. Kidney histology was analyzed by hematoxylin and eosin, periodic acid-Schiff, and immunohistochemical staining.

## RESULTS

Fluorescence imaging confirmed that MSCs transferred mitochondria to injured GECs when co-cultured *in vitro*. We found that the apoptosis, proliferation, and mitochondrial function of injured GECs were improved following co-culture. Additionally, MSCs decreased pro-inflammatory cytokines [interleukin (IL)-6, IL-1 $\beta$ , and tumor necrosis factor- $\alpha$ ] and pro-apoptotic factors (caspase 3 and Bax). Mitochondrial transfer also enhanced the expression of superoxide dismutase 2, B cell lymphoma-2, glutathione peroxidase (GPx) 3, and mitofusin 2 and inhibited reactive oxygen species (ROS) and dynamin-related protein 1 expression. Furthermore, MSCs significantly ameliorated functional parameters (blood urea nitrogen and serum creatinine) and decreased the production of malondialdehyde, advanced glycation end products, and ROS, whereas they increased the levels of GPx and superoxide dismutase *in vivo*. In addition, significant reductions in the glomerular basement membrane and renal interstitial fibrosis were observed following MSC treatment.

## CONCLUSION

MSCs can rejuvenate damaged GECs *via* mitochondrial transfer. Additionally, the improvement of renal function and pathological changes in DKD by MSCs may be related to the mechanism of mitochondrial transfer.

**Key Words:** Mitochondria transfer; Mesenchymal stem cells; Glomerular endothelial cells; Diabetic kidney disease; Mitochondrial dysfunction; Oxidative stress

©The Author(s) 2022. Published by Baishideng Publishing Group Inc. All rights reserved.

**Core Tip:** This study demonstrated that the MitoTracker Red CMXRos labeled mitochondria were transferred from mesenchymal stem cells (MSCs) to the high glucose-injured glomerular endothelial cells (GECs) *in vitro*. Additionally, GEC proliferation was enhanced, and GEC apoptosis was suppressed. Furthermore, *in vivo* experiments showed that MSCs ameliorated renal function damage and pathological progression of diabetic kidney disease (DKD). These data suggest that MSCs may rescue damaged GECs and improve the renal function and pathological changes of DKD partly through mitochondrial transfer.

**Citation:** Tang LX, Wei B, Jiang LY, Ying YY, Li K, Chen TX, Huang RF, Shi MJ, Xu H. Intercellular mitochondrial transfer as a means of revitalizing injured glomerular endothelial cells. *World J Stem Cells* 2022; 14(9): 729-743

**URL:** <https://www.wjgnet.com/1948-0210/full/v14/i9/729.htm>

**DOI:** <https://dx.doi.org/10.4252/wjsc.v14.i9.729>

## INTRODUCTION

The prevalence of diabetic kidney disease (DKD), also known as diabetic nephropathy, is increasing worldwide. The global all-age mortality rate from chronic kidney disease (CKD) increased by 41.5% between 1990 and 2017[1]. Additionally, CKD caused the death of 1.2 million people in 2017 and there was an increase of 697.5 million cases of all-stage CKD[1]. Furthermore, a decomposition analysis showed that the burden of DKD accounted for about half the increase in CKD disability-adjusted life years[2]. Due to the high mortality rate, morbidity, and financial burden, DKD is an urgent public health issue.

Amongst the many known mechanisms of DKD pathophysiology, the mechanism of mitochondrial dysfunction appears to play an essential role in its development[3,4]. Mitochondria play vital roles in biological processes such as oxidative phosphorylation, cellular metabolism, and cell death[5]. Recent studies indicate that mitochondrial damage occurs in glomerular endothelial cells (GECs) and podocytes in DKD[6,7]. Moreover, hyperglycemia results in mitochondrial dysfunction[8], which produces an excessive amount of reactive oxygen species (ROS), especially in GECs[6].

Mesenchymal stem cells (MSCs) have the potential to treat diabetes-related complications. However, their therapeutic effects and mechanisms of action have not been determined as of yet. Notably, a

possible benefit of stem cells might be their ability to release mitochondria[9]. Transferring mitochondria from human bone marrow MSCs (BMSCs) to human umbilical cord vein endothelial cells (HUVECs) has been suggested to reduce apoptosis, stimulate proliferation, and restore transmembrane migration in injured HUVECs[10]. In streptozotocin (STZ)-induced diabetic animals, Konari reported the transfer of mitochondria from systemically administered BMSCs to renal proximal tubular epithelial cells (PTECs)[11]. Moreover, when BMSCs transferred their mitochondria to lung epithelial cells[12] and cardiomyocytes[13], they resulted in increased adenosine triphosphate (ATP) levels and apoptosis suppression. In addition, MSCs' mitochondria can be transferred to myocardial cells[14], alveolar epithelial cells[15], and astrocytes[16], which restore cellular oxidative respiratory function and reduce apoptosis. Therefore, a new concept for cell-cell signals involving intercellular mitochondrial transfer is now proposed[9]. Because the pathological changes in many tissues are related to the impairment of mitochondrial function, replacing dysfunctional mitochondria with healthy donor mitochondria has broad research applications[16]. Supplementing exogenous healthy mitochondria to replace damaged mitochondria can improve the bioenergetics of damaged cells, reverse excessive ROS production, and restore mitochondrial function[17]. However, experimental data on how stem cells influence injured GEC mitochondria is limited.

Previous studies have focused on glomerular hyper-filtration, oxidative stress, advanced glycation end products (AGEs), activation of intracellular signaling pathways, and epigenetic changes in the pathogenesis of DKD[2]. However, dysregulation of mitochondrial metabolism leads to the occurrence and progression of DKD[7,18]. The importance of MSCs in glomerular development is still highly debated, but one theory is that MSCs provide an environment conducive to glomerular development. Further investigation of the mechanisms of action of MSCs should be conducted, particularly those that involve the interaction between GECs and grafted MSCs. This study was designed to determine if MSCs could repair GECs with dysfunctional mitochondria by transferring their mitochondria. This research supports the idea that stem cell mitochondrial transfer can treat DKD or other diseases with mitochondrial dysfunction.

## MATERIALS AND METHODS

### **Cell cultures and cell lines**

BMSCs were isolated from Sprague-Dawley rats (4-6 wk old) using the adherence exclusion method following previously published protocols[19]. The isolated cells were resuspended in endothelial cell medium (ECM) (ScienCell, California, United States) containing 10% (v/v) fetal bovine serum (FBS) (ScienCell) and 1% (v/v) penicillin-streptomycin (P/S) (ScienCell), and then incubated at 37 °C with 5% circulating CO<sub>2</sub>. BMSCs at passages 2-4 were used in the following experiments. GECs were purchased (ScienCell) and cultured in ECM containing 10% FBS, 1% P/S, and 1% (v/v) endothelial cell growth supplement (ScienCell). GECs at passages 2-3 were used in the following experiments.

BMSCs were identified by differentiation potential and fluorescence-activated cell sorting (FACS) to evaluate the cell surface markers. BMSCs could be differentiated into osteogenic, adipogenic, and chondrogenic phenotypes when incubated in an osteogenic-, adipogenic-, or chondrogenic-inducing medium (Cyagen, Suzhou, China) according to the manufacturer's instructions. Osteogenic, adipogenic, and chondrogenic differentiation capacity of BMSCs was observed using Alizarin red staining, Oil red O staining, and Alcian Blue staining, respectively, and photographed under the light microscope (Olympus, Tokyo, Japan). The results are shown in [Supplementary Figures 1A-C](#). The BMSCs were incubated with PE-conjugated CD45 polyclonal antibody (BD Biosciences, United States) and fluorescein isothiocyanate (FITC)-conjugated CD44 polyclonal antibody (BD Biosciences). The BMSCs expressed the antigen CD44 but not CD45 ([Supplementary Figure 1D](#)).

### **Cell label and co-culture model**

The mitochondria of GECs and BMSCs were labeled to detect mitochondrial transfer before co-cultivation. GEC cells ( $5 \times 10^5$  cells) were first incubated with 200 nmol/L MitoTracker Green (Beyotime, Shanghai, China) for 25 min at 37 °C with 5% CO<sub>2</sub>, and then the nuclei were stained with Hoechst 33342 (Beyotime). BMSCs ( $5 \times 10^5$  cells) were incubated with 200 nmol/L MitoTracker Red CMXRos (Beyotime) for 30 min, and then co-cultured with GECs in a 1:1 ratio and incubated at 37 °C with 5% CO<sub>2</sub>. GECs were pre-cultured in ECM complete medium supplemented with high D-glucose (30 mmol/L; Sigma, United Kingdom) for 24 h to induce stress. Cells were randomly divided into four groups: (1) Normal control (NC) group: ECM complete medium containing D-glucose (5.5 mmol/L); (2) NC + MSC group; (3) High glucose (HG) group: D-glucose (30 mmol/L); and (4) HG + MSC group. A fluorescence microscope (Olympus) was used to examine live cells after 48 h of co-culture. For further analysis, supernatants and cells were collected.

### **Flow cytometry and cell sorting**

To examine the protective effects on the injured GECs, FACS Aria III analysis (BD Biosciences) was used on at least  $2 \times 10^7$  co-cultured cells after 48 h. GECs requiring sorting were pre-labeled with

CellTracker™ Violet (CTV) (Invitrogen, United States). Sorting and purification were performed based on CTV-positive labeled cells. Following the cell sorting, GECs were tested for apoptosis, viability, ROS measurement, protein expression by western blot, and mitochondrial function.

### **Measurement of cell apoptosis and viability**

Annexin V-FITC/Propidium Iodide (PI) Apoptosis Detection Kit (Beyotime) was used to determine apoptosis after co-culturing for 48 h. The sorted GECs were resuspended in 195  $\mu$ L Annexin-binding buffer according to the manufacturer's instructions. In brief, approximately 5  $\mu$ L of Annexin V-FITC working solution and 10  $\mu$ L of PI were added to a  $1 \times 10^5$  cell suspension in darkness over 20 min. The fluorescence intensity was analyzed by BD FACSCelesta (BD Biosciences) within 1 h. Annexin V-FITC or PI staining results were calculated to indicate the early or late stages of apoptosis, respectively.

The cell viability was estimated using the Cell Counting Kit-8 (CCK-8) (Beyotime). GECs were plated in 10  $\mu$ L of CCK-8 and incubated for 2 h in 96-well microplates filled with culture medium. A fluorescent microplate reader (FLx800™, BioTek, United States) was used to take readings at 450 nm, and a decrease in optical density was interpreted as a decrease in viability.

### **Assessment of ATP production**

A luciferin-luciferase bioluminescence assay was used to assess ATP production. Briefly, the sorted GEC cells were collected, subjected to a single freeze-thaw cycle, and centrifuged. To measure ATP levels, supernatants were collected using an ATP determination kit (Invitrogen), following instructions from the kit manufacturer and the published protocol[20]. Standard curves normalized with protein concentrations (nmol/L ATP/ $\mu$ g protein) were used to calculate the ATP concentration.

### **Mitochondrial membrane potential**

Mitochondrial membrane potential ( $\Delta \Psi_m$ ) was examined in live cells with the enhanced mitochondrial membrane potential assay kit (JC-1) (Beyotime). Briefly,  $6 \times 10^5$  GEC cells were incubated with 0.5 mL JC-1 ( $1 \times$ ) working solution in complete culture medium for 30 min at 37 °C and centrifuged at 600 g for 3 min. Then, the cells were resuspended with 1 mL JC-1 staining buffer. Carbonyl cyanide 3-chlorophenylhydrazone (10  $\mu$ mol/L; Beyotime) treated cells were used as a positive control. The fluorescence intensity was analyzed by BD FACSCelesta (BD Biosciences) for quantitative analysis.

### **ROS and interleukin-6 measurement**

Intracellular ROS and mitochondrial ROS were measured using flow cytometry, following cell staining with a DCF-DA probe (Beyotime) and MitoSOX™ Red fluorescent probe (Invitrogen), respectively. Freshly sorted GEC cells were seeded in a 48-well plate at a density of  $1 \times 10^4$  cells per well and then cultured in a growth medium for 12 h to completely adhere to the wall surface. Cell pellets were collected after staining with DCF-DA (5  $\mu$ mol/L) or MitoSOX™ Red (5  $\mu$ mol/L) for 30 min at 37 °C, and fluorescence was detected with a flow cytometer. The level of interleukin (IL)-6 was measured according to the manufacturer's instructions for the enzyme-linked immunosorbent assay (ELISA) kit (Invitrogen).

### **RNA extraction and real-time reverse transcriptase-polymerase chain reaction**

Real-time reverse transcriptase-polymerase chain reaction (RT-qPCR) was used to detect caspase 3, B cell lymphoma (*Bcl*)-2, *Bax*, tumor necrosis factor (*TNF*)- $\alpha$ , and *IL-1 $\beta$*  mRNA expression levels. Briefly, total RNA was isolated from cells or kidney tissues using Trizol reagent (Beyotime). With the Applied Biosystems™ 7500 RT-qPCR System (Thermo Fisher Scientific), RNA reverse transcription was performed with the SuperScript III (Invitrogen), followed by RT-qPCR with SYBR Green MasterMix. GAPDH served as an internal control. All samples were analyzed in triplicate. RT-qPCR results were analyzed by the  $2^{-\Delta\Delta Ct}$  method and then converted to fold changes. All primer sequences were obtained from publications[21-24] and commercially synthesized (Servicebio, Wuhan, China), and the utilized sequences are shown in [Supplementary Table 1](#).

### **Western blot analysis**

After extracting the proteins with RIPA buffer and protease inhibitor, the total protein contents were measured using a BCA assay kit (Servicebio). By normalizing protein content, all samples had the same quality and volume for further analysis. A wet-transfer method was used to separate proteins by 10% or 12% sodium dodecyl sulfate polyacrylamide gel electrophoresis and transfer them to polyvinylidene fluoride membranes. The membranes were blocked in pure methanol before use and then blocked in  $1 \times$  TBS containing 3% bovine serum albumin (Solarbio, Beijing, China). The membranes were then incubated overnight with primary antibodies: Anti-Bax (GB11690; Servicebio), anti-Bcl-2 (ab196495; Abcam), anti-caspase-3 (GB11767C; Servicebio), anti-superoxide dismutase 2 (SOD2) (GB111875; Servicebio), anti-glutathione peroxidase 3 (GPx-3) (ab256470; Abcam), anti-dynamin-related protein 1 (DRP1) (8570S; CST), anti-mitofusin 2 (MFN2) (ab124773; Abcam), and anti- $\beta$ -Actin (GB15001; Servicebio) antibodies. After washing with TBS-T, they were incubated with appropriately diluted horseradish peroxidase (HRP) conjugated Goat Anti-Rabbit immunoglobulin (Ig)G (GB23303;

Servicebio) or HRP conjugated Goat Anti-Mouse IgG (GB23301; Servicebio) as the secondary antibody. Protein bands were visualized using the BeyoECL Moon chemiluminescence system (Beyotime).

### **Animal study**

All animal methods were carried out following the National Institutes of Health Guidelines for the care and use of laboratory animals and were handled according to protocols approved by the Animal Experimental Ethical Committee of Southeast University (Nanjing, China). Eight-week-old male Sprague-Dawley rats were obtained from Southeast University Laboratory Animal Centre, and diabetes was induced by a single intraperitoneal injection of 60 mg/kg of STZ (Sigma-Aldrich, United States) dissolved in 10 mmol/L citrate buffer (pH 4.5), as our previously published study[25]. To verify the successful establishment of the diabetes model, fasting blood glucose (FBG) levels ( $\geq 16.7$  mmol/L) were measured for three consecutive days after STZ administration for 3 d. The diabetic rats were provided with standard rat food for 4 wk. An excretion rate of  $> 30$  mg of 24-h urinary albumin (U-Alb) was observed at week 4, suggesting successful DKD induction[26].

DKD rats were randomly divided into two groups ( $n = 5$ ). Group 1 was treated with  $2 \times 10^6$  MSCs (pre-labeled with 200 nmol/L MitoTracker Red CMXRos) dissolved in 100  $\mu$ L Hank's Balanced Salt Solution (HBSS) (DKD + MSC group), and group 2 received HBSS (DKD group) by tail vein injection. Five non-diabetic rats served as a normal control group (NC group). Rats were sacrificed 2 wk after treatment for biochemical and histological analyses.

### **Evaluation of FBG, 24 h U-Alb, serum blood urea nitrogen, serum creatinine, and AGE levels**

The levels of FBG were measured before and after each STZ injection. Samples obtained from the tail vein were tested for FBG using a blood glucose meter (LifeScan, CA, United States). Metabolic cages were used to collect 24-h urine from rats. The levels of 24 h U-Alb, blood urea nitrogen (BUN), and serum creatinine (Scr) were measured using an AU2700 automatic biochemical analyzer (Olympus). AGE level was measured according to the ELISA kit's instructions (Cusabio, China).

### **Assessment of SOD, malondialdehyde, and GPx in kidney tissue**

A homogenizer was used to homogenize approximately 100 mg of kidney tissue in 5% phosphate-buffered saline. After centrifugation, the clear supernatant was collected. SOD values were measured with the xanthine oxidase activity assay kit (Sigma-Aldrich), the malondialdehyde (MDA) level was measured by the thiobarbituric acid method (MDA colorimetric assay kit; Elabscience, China), and a colorimetric assay kit (Elabscience) was used to measure the GPx concentration, following the manufacturer's protocol.

### **Histological analysis**

Rat kidneys were dissected and fixed in 4% paraformaldehyde and embedded in paraffin, and 4  $\mu$ m serial sections were then prepared for histological analysis under a light microscope or fluorescence microscope. TdT-mediated dUTP nick-end labeling (TUNEL) was done with an apoptosis detection kit (Servicebio) following the manufacturer's instructions. Hematoxylin and eosin (HE) staining and periodic acid-Schiff (PAS)[27] staining were carried out using standard protocols. A random sample of three glomeruli from each rat was analyzed using image analysis software (Image-Pro plus 6.0) to determine the percentage of PAS-positive areas, expressed as a mesangial index. Immunohistochemical (IHC) analyses were carried out using the rabbit anti-AGEs (1:300; bs-1158R; Bioss, Woburn, MA, United States) primary antibodies. HRP-conjugated goat anti-rabbit IgG (1:500; GB23303; Servicebio) was used to detect primary antibodies. The nuclei were subsequently stained with 3,3'-diaminobenzidine, and three fields of view from each rat were digitized. The integrated optical density from all fields was calculated using Image-Pro Plus 6.0.

### **Statistical analysis**

Data are presented as the mean  $\pm$  SD based on at least three independent experiments. Statistical analyses were conducted using IBM SPSS 26.0 (Chicago, IL, United States). Comparing multiple groups was done using one-way analysis of variance, followed by Bonferroni's *post hoc* test. The significance of the data was defined at  $P < 0.05$ .

## **RESULTS**

### **Transfer of mitochondria from MSCs to GECs alleviates high glucose-induced GEC apoptosis and promotes GEC proliferation**

As a visual demonstration of mitochondrial transfer, the mitochondria of the GECs and the BMSCs were labeled with MitoTracker Green and MitoTracker Red CMXRos, respectively, and the nuclei of GECs were labeled with Hoechst 33342 before co-cultivation. CMXRos-labeled mitochondria were rarely transferred from MSCs to NC-GECs. However, CMXRos-mitochondria of MSCs were markedly

transferred into HG-induced damaged GECs *in vitro* (Figure 1A).

To further confirm that mitochondrial transfer is involved in protecting GECs, RT-qPCR, CCK-8, western blot, and flow cytometry assays were performed. The mRNA and protein expression levels of caspase 3 and Bax in the HG group were dramatically higher than those in the control group (Figures 1B and C). Interestingly, treatment with MSCs significantly inhibited this upregulation (Figures 1B and C). The changes observed in the mRNA and protein expression of Bcl-2 were opposite to those observed for Bax and caspase 3 (Figures 1B and C). The ratio of Bcl-2/Bax increased in the HG + MSC group compared to that in the HG group, although it was not statistically significant. Flow cytometry with Annexin V-FITC/PI staining and CCK-8 assay was used to detect cell apoptosis and viability, respectively. From these assessments, we observed that HG treatment significantly reduced the cell viability of cultured GECs and increased their apoptosis (NC *vs* HG:  $0.533 \pm 0.053$  *vs*  $0.336 \pm 0.043$ ,  $P < 0.001$ ). In contrast, MSC co-culture significantly reversed these outcomes (HG *vs* HG + MSC:  $0.3358 \pm 0.043$  *vs*  $0.439 \pm 0.05$ ,  $P < 0.01$ ) (Figures 1D and E). These results suggest that mitochondrial transfer plays a notable role in the anti-apoptotic mechanisms of MSCs.

### **Mitochondrial transfer alleviates mitochondrial activity and oxidative stress in high glucose-induced GECs**

To evaluate the mitochondrial activity of GECs, *in vitro* co-culture experiments were performed. CTV-positive GECs were sorted by flow cytometry. Compared with the HG-induced GECs group, the ATP production of MSC-treated GECs was significantly upregulated ( $5.59 \pm 0.58$  *vs*  $6.91 \pm 0.84$ ,  $P < 0.05$ ) (Figure 2A). Additionally, staining with the  $\Delta\Psi_m$  indicator, JC-1, revealed significant attenuation of GECs by flow cytometry at 48 h (HG *vs* HG + MSC:  $69.21 \pm 5.06$  *vs*  $80.44 \pm 6.49$ ,  $P < 0.05$ ) (Figure 2B).

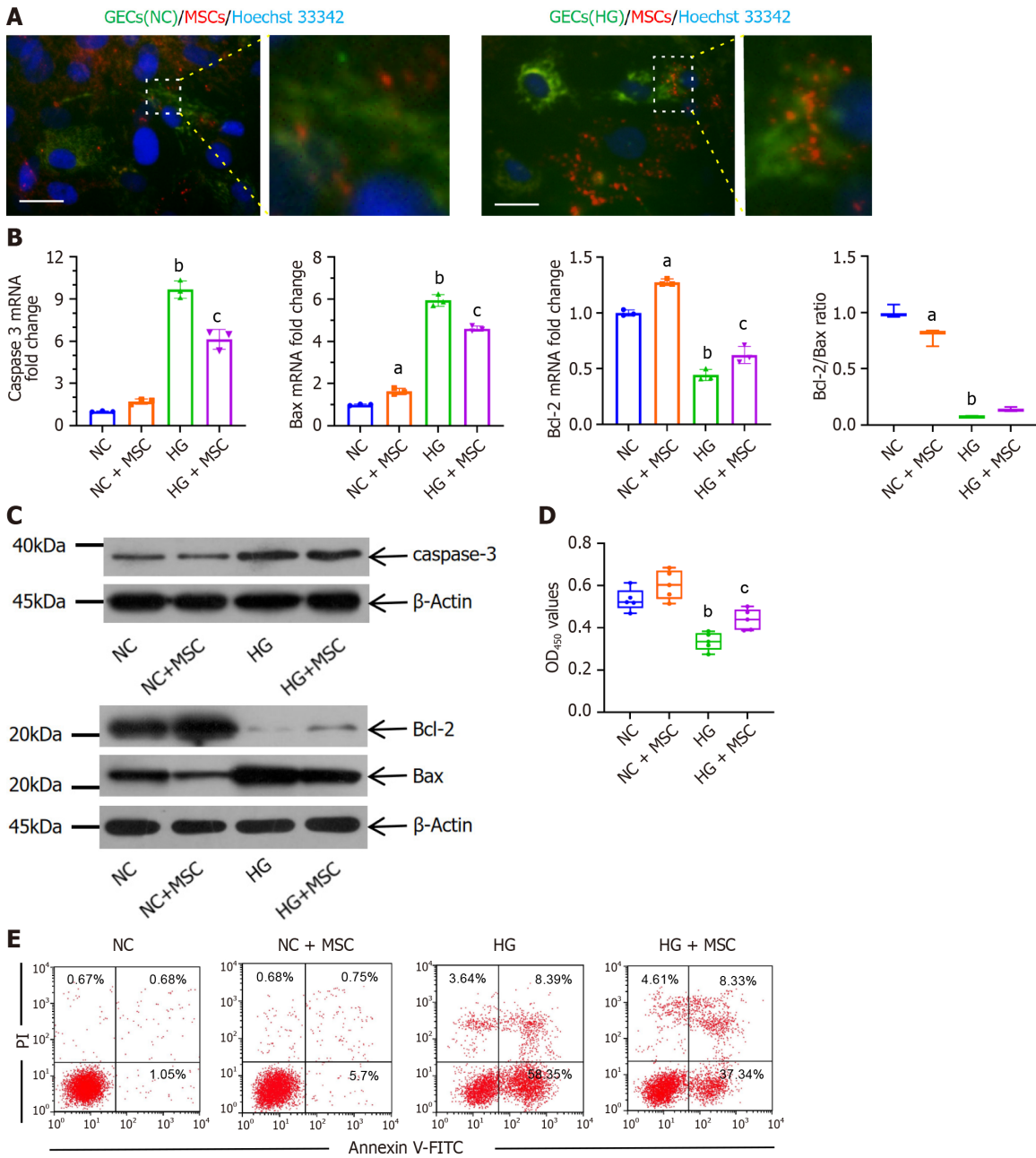
To determine the impact of mitochondrial transfer on mitochondrial dynamics, the protein levels of mitochondrial fission factor (DRP1) and fusion factor (MFN2) were analyzed. Representative western blots showed that treatment with MSCs decreased the level of DRP1, whereas MFN2 level increased (Figure 2C). In addition, intracellular and mitochondrial ROS production was visualized using DCF-DA and MitoSOX Red ROS indicators, respectively. Compared with NC-GECs, HG significantly increased DCF-DA and MitoSOX Red fluorescent intensity, suggesting high levels of ROS. In contrast, pretreatment with MSCs attenuated HG-induced upregulation in ROS levels (Figure 2D). Moreover, the expression levels of ROS-protective enzymes (SOD2 and GPx-3) increased after MSC treatment of HG-induced GECs (Figure 2E). We then analyzed the expression of inflammatory cytokines in GECs cultured with or without MSCs to characterize the mechanism of mitochondrial transfer on HG-GECs. The expression of the inflammatory cytokines TNF- $\alpha$ , IL-1 $\beta$ , and IL-6 decreased significantly in the HG-GECs cultured with MSCs for 48 h. In contrast, the addition of MSCs did not affect the expression of these inflammation cytokines in NC-GECs (Figures 2F and G). The above results demonstrate that direct co-culture with MSCs improved the capacity of GECs to resist oxidative stress.

### **MSC treatment improves renal function and relieves inflammation of DKD rats**

An animal model of STZ-induced DKD was established to explore the therapeutic effect of MSCs on DKD. Following MSC treatment for 2 wk, the rats were sacrificed (5/5 in each group), and tissue specimens were collected for further analysis (Figure 3A). The FBG and 24 h U-Alb levels of the DKD and DKD + MSC groups were significantly higher than those of the NC group. There was no statistically significant increase in FBG or 24 h U-Alb in the MSC group relative to the DKD group, although the levels showed a trend towards an increase (Figure 3B). Significantly higher serum BUN and Scr were found in the DKD group than in the control group, but MSC treatment significantly reduced these changes (Figure 3C). RT-qPCR was applied to evaluate the expression of apoptosis-related genes. Compared with the NC group, caspase 3 and Bax expression in DKD rats was significantly increased, suggesting increased pro-apoptotic mechanisms (Figure 3D). In contrast, MSC injection reduced the expression of the pro-apoptotic markers caspase 3 and Bax. However, changes in the expression of Bcl-2 were increased (Figure 3D). The ratio of Bcl-2/Bax increased in the DKD + MSC group compared to the DKD group, although the difference was not statistically significant. The levels of MDA (a marker of lipid peroxidation/oxidative stress) and AGEs (contribute to oxidative stress) were lower in the NC group than in the other groups (Figure 3E). MSCs significantly decreased AGEs and MDA in DKD rats (Figure 3E). Notably, the levels of GPx (a marker of oxidative stress) in each group were inversely (DKD *vs* DKD + MSC:  $2.08 \pm 0.29$  *vs*  $2.67 \pm 0.2$ ,  $P < 0.05$ ) (Figure 3E). We then used DCF probes and the xanthine oxidase activity assay kit to evaluate the ROS generation and scavenging ability. ROS production decreased in the DKD group while SOD level increased after MSC administration (Figure 3F). Overall, these results suggest that MSCs can ameliorate the abnormal renal function of DKD rats.

### **MSC treatment ameliorates renal pathological changes**

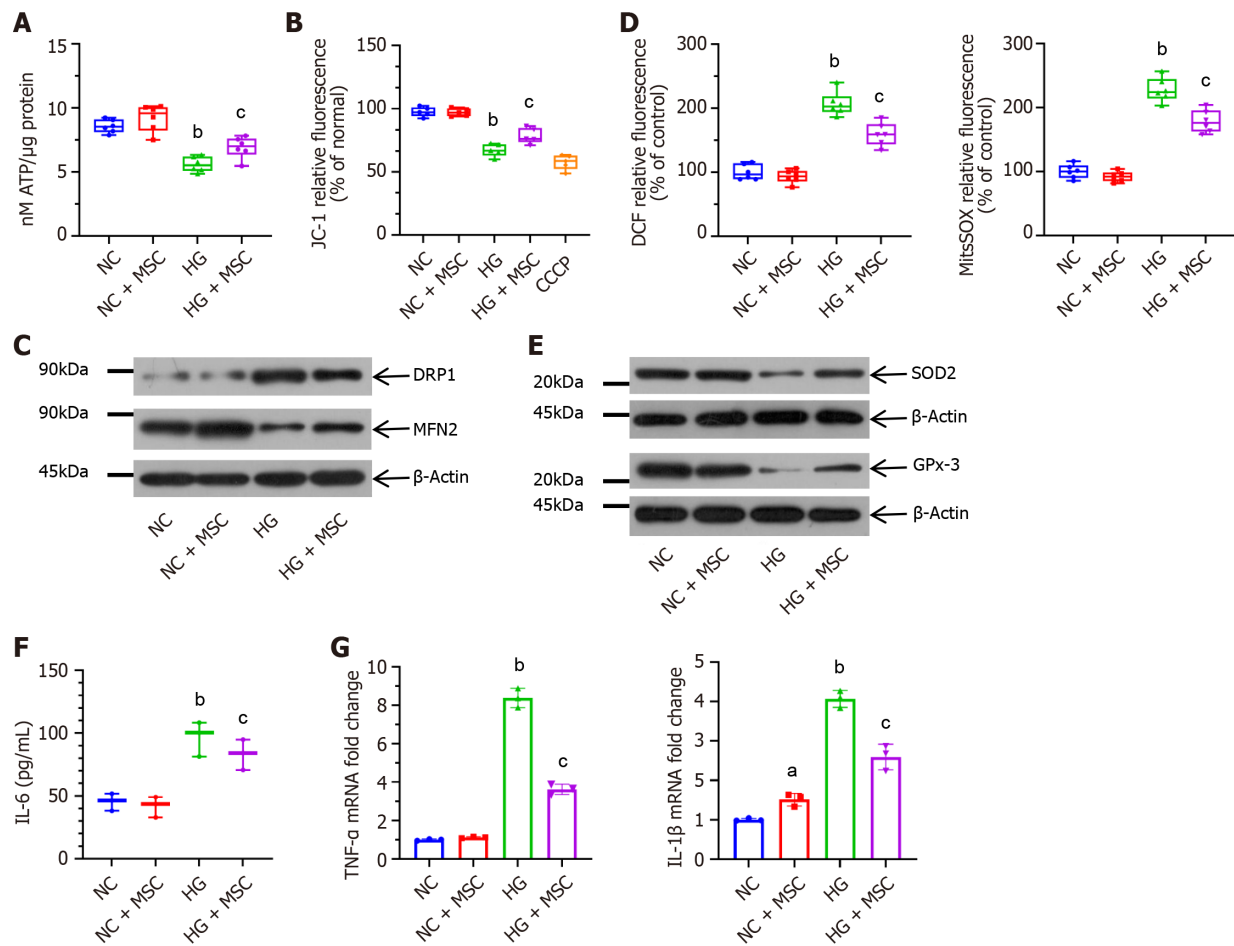
As shown in Figure 4, TUNEL, HE, PAS, and IHC staining (5/5 in each group) were performed on kidney tissue sections from selected experimental groups. The TUNEL method was used to investigate the apoptotic cells in renal tissue. Figure 4A shows that the number of TUNEL-positive apoptotic cells in kidney tissue of DKD rats was increased, while their positive expression was decreased after injection of



DOI: 10.4252/wjsc.v14.i9.729 Copyright ©The Author(s) 2022.

**Figure 1** Anti-apoptotic effects of mesenchymal stem cells on high glucose-induced glomerular endothelial cells *in vitro*. **A:** Immunofluorescence images of MitoTracker green (green) labeled normal control-glomerular endothelial cells (NC-GECs) and high glucose-induced GECs (HG-GECs) cultured with MitoTracker Red CMXRos (red) labeled mesenchymal stem cells (MSCs). GEC nuclei were counterstained with Hoechst 33342 (blue). A few spontaneous mitochondria transferred from MSCs to NC-GECs. Interestingly, a robust transfer of numerous mitochondria from MSCs to HG-GECs was observed. Scale bar: 200 nm; **B:** Caspase 3, *Bax*, and B-cell lymphoma 2 mRNA expression detected by real-time reverse transcriptase-polymerase chain reaction; **C:** Caspase 3, *Bax*, and B-cell lymphoma 2 protein expression detected by western blot; **D:** GEC viability assays performed using the Cell Counting Kit-8; **E:** Cellular apoptosis analysis in GEC cells treated with MSCs using Annexin V-FITC/PI staining. Data are presented as the mean ± SD. <sup>a</sup>*P* < 0.05 vs normal control group, <sup>b</sup>*P* < 0.01 vs normal control group, <sup>c</sup>*P* < 0.05 vs high glucose-induced group. GECs: Glomerular endothelial cells; MSCs: Mesenchymal stem cells; NC-GECs: Normal control glomerular endothelial cells; HG-GECs: High glucose-induced GECs; Bcl-2: B-cell lymphoma 2.

MSCs. In the DKD group, HE staining revealed an inflammatory cell infiltration in the renal tissue (Figure 4B). Additionally, PAS staining showed severe glomerular and tubular changes in the DKD group. Atrophied glomeruli, ectopic mesangial extracellular matrix, high glycogen levels, kidney interstitial fibrosis, and basement membrane thickening were also observed (Figure 4C). The DKD group showed a degenerative phenotype indicative of glomerular endothelial degeneration by HE and PAS staining, while MSC therapy alleviated these pathological changes (Figures 4B and C). Compared to the NC group, the DKD and DKD + MSC groups showed significant increases in the mesangial index (58.69 ± 11.7 vs 195.13 ± 32.55, *P* < 0.001; 58.69 ± 11.7 vs 160.67 ± 29.12, *P* < 0.001; respectively) (Figure 4D). The mesangial index in the DKD + MSC group was markedly lower than that of the DKD



DOI: 10.4252/wjsc.v14.i9.729 Copyright ©The Author(s) 2022.

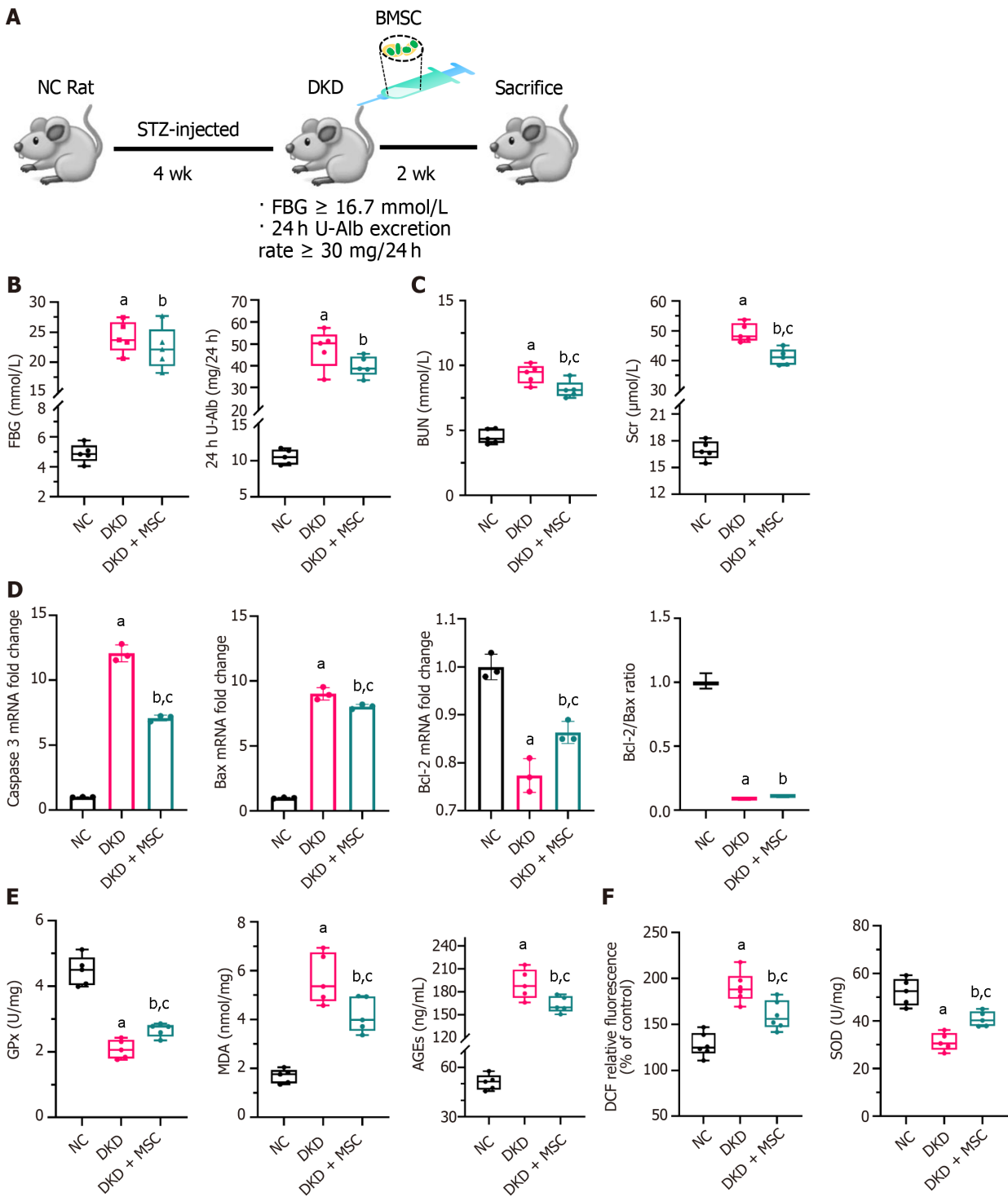
**Figure 2 Mesenchymal stem cells alleviate mitochondrial activity and high glucose-induced oxidative stress in cultured glomerular endothelial cells.** A: Mesenchymal stem cells (MSCs) increased adenosine triphosphate production in high glucose (HG)-induced glomerular endothelial cells (GECs); B: MSCs also attenuated mitochondrial membrane potential ( $\Delta \Psi_m$ ) in GECs. Carbonyl cyanide 3-chlorophenylhydrazone as a mitochondrial oxidative phosphorylation uncoupler, was used as the positive control group; C: Effect on mitochondrial fission marker and the fusion marker levels; D: Pretreatment with MSCs attenuated HG-induced upregulation in DCF-DA [intracellular reactive oxygen species (ROS)] and MitoSOX Red (mitochondrial ROS) fluorescent intensity; E: Representative western blot expression levels of ROS-protective enzymes (superoxide dismutase 2 and glutathione peroxidase 3); F: Concentration of interleukin (IL)-6 in the supernatant by enzyme-linked immunosorbent assay; G: Mitochondrial transfer ameliorated the mRNA expression levels of inflammatory markers (tumor necrosis factor- $\alpha$  and IL-1 $\beta$ ), as determined using real-time reverse transcriptase-polymerase chain reaction. Data are presented as the mean  $\pm$  SD. <sup>a</sup> $P < 0.05$  vs normal control group, <sup>b</sup> $P < 0.01$  vs normal control group, <sup>c</sup> $P < 0.05$  vs high glucose group. MSCs: Mesenchymal stem cells; DRP1: Dynamin-related protein 1; MFN2: Mitofusin 2; ROS: Reactive oxygen species; SOD2: Superoxide dismutase 2; GPx-3: Glutathione peroxidase 3; IL-6: Interleukin-6; CCCP: Carbonyl cyanide 3-chlorophenylhydrazone; NC: Normal control; HG: High glucose; TNF- $\alpha$ : Tumor necrosis factor- $\alpha$ ; ATP: Adenosine triphosphate.

group ( $160.67 \pm 29.12$  vs  $195.13 \pm 32.55$ ,  $P < 0.01$ ). Figures 4E and F illustrates the kidney expression of AGEs as detected by IHC. A deficient level of staining signals was observed around the renal corpuscle wall and the tubular basement membrane in the NC group. Interestingly, the DKD group showed higher expression of AGEs than the NC group ( $64.53 \pm 15.86$  vs  $8.58 \pm 3.83$ ,  $P < 0.001$ ) or DKD + MSC group ( $64.53 \pm 15.86$  vs  $52.62 \pm 10.33$ ,  $P < 0.05$ ). Notably, the DKD + MSC group showed significantly decreased staining signals around the capsule and on the tubular basement membrane.

## DISCUSSION

Recently, the administration of BMSCs has been shown to accelerate kidney reconstitution[28,29]. However, the underlying mechanism of action of MSCs that promote DKD kidney reconstitution is not yet fully understood. Apoptosis of GECs induced by mitochondrial dysfunction is suggested to play a role in the development of DKD. Therefore, one potential mechanism in BMSC-mediated kidney reconstitution is *via* BMSC and GEC cell-cell communication, resulting in the rescue of the injured GECs and promoting kidney reconstitution. MSCs can repair injuries in various ways, including secreting paracrine factors, transferring proteins and RNA, and transferring organelles such as mitochondria[30]. In this study, we demonstrated a novel mechanism of MSCs that they can transfer functional



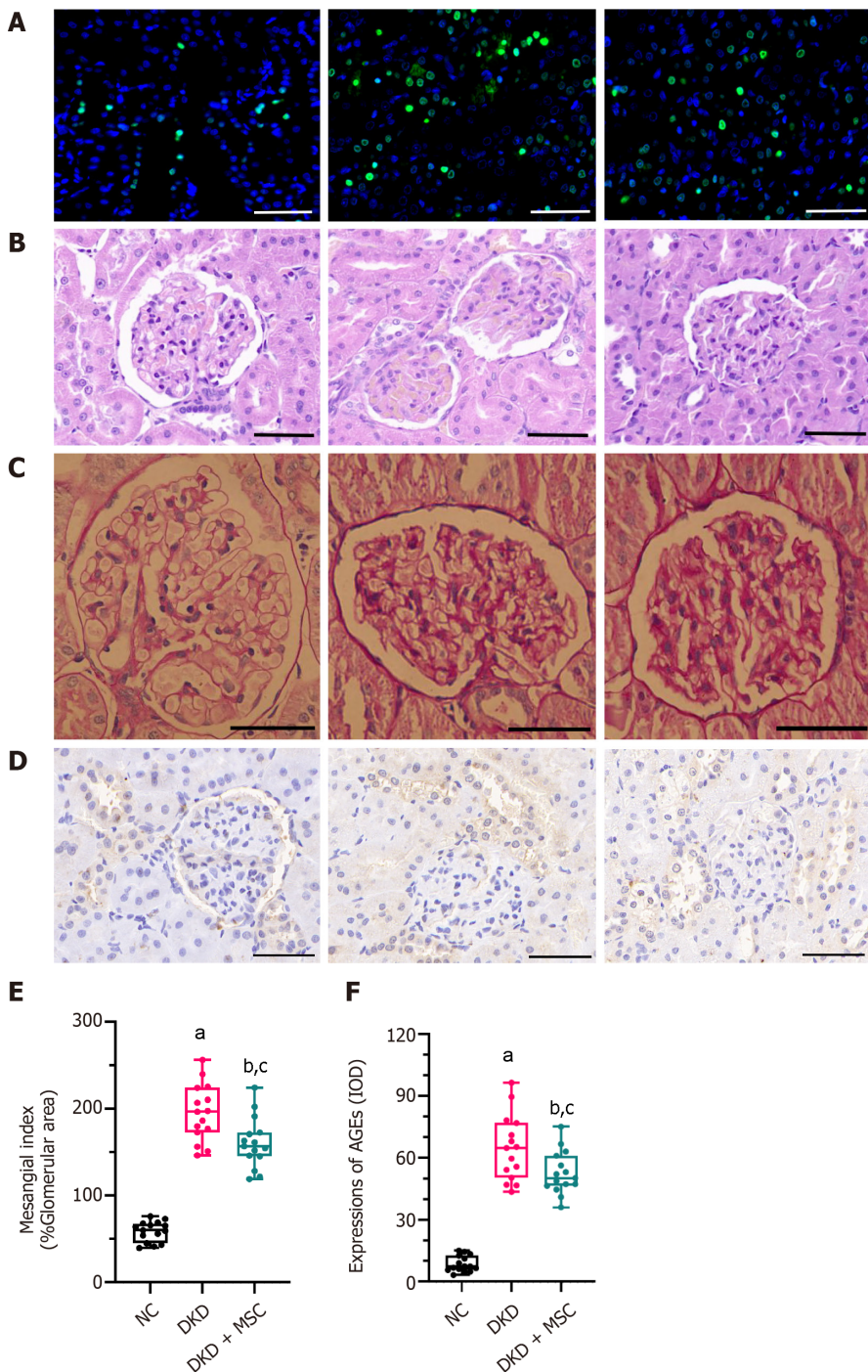


DOI: 10.4252/wjsc.v14.i9.729 Copyright ©The Author(s) 2022.

**Figure 3** Effects of mesenchymal stem cell treatment on biochemical indexes. A: Flowchart of rat treatment from day 0 to week 6; B: Fasting blood glucose and 24-h urinary albumin concentration; C: Concentrations of blood urea nitrogen and serum creatinine in rat serum; D: Relative mRNA expression of caspase 3, *Bax*, and B-cell lymphoma 2 (*Bcl-2*), and *Bcl-2/Bax* ratio in rat kidney tissues; E: Concentrations of glutathione peroxidase, malondialdehyde, and advanced glycation end products in rat kidney tissues; F: Levels of reactive oxygen species and superoxide dismutase in kidney tissues. Data are presented as the mean ± SD. <sup>a</sup>*P* < 0.001 vs normal control group, <sup>b</sup>*P* < 0.01 vs normal control group, <sup>c</sup>*P* < 0.05 vs diabetic kidney disease group. NC: Normal control; FBG: Fasting blood glucose; 24 h U-Alb: 24-h urinary albumin; BUN: Blood urea nitrogen; Scr: Serum creatinine; *Bcl-2*: B-cell Lymphoma 2; *Bax*: BCL2-Associated X; GPx: Glutathione peroxidase; AGEs: Advanced glycation end products; MDA: Malondialdehyde; SOD: Superoxide dismutase; NC: Normal control; DKD: Diabetic kidney disease; MSCs: Mesenchymal stem cells.

mitochondria into GECs *in vitro*. Therefore, the therapeutic effects of BMSC on DKD rats may be related to the mechanism of mitochondrial transfer.

From our investigations, fluorescent imaging revealed that CMXRos-labeled mitochondria were transferred extensively from MSCs to HG-induced stressed GECs. As previously reported, the



DOI: 10.4252/wjsc.v14.i9.729 Copyright ©The Author(s) 2022.

**Figure 4** TdT-mediated dUTP nick-end labeling and histopathology analysis of kidney tissues from all rats. A: TdT-mediated dUTP nick-end labeling staining. Nuclei: Blue; apoptosis: Green; B: Hematoxylin-eosin staining; C: Periodic acid-Schiff (PAS) staining; D: Mesangial index of PAS-positive areas in the glomerulus; E: Immunohistochemical staining of advanced glycation end products (AGEs); F: Integrated optical density of AGEs in kidney tissues. All scale bar: 50  $\mu$ m. Data are presented as the mean  $\pm$  SD. <sup>a</sup>*P* < 0.001 vs normal control group, <sup>b</sup>*P* < 0.001 vs normal control group, <sup>c</sup>*P* < 0.05 vs diabetic kidney disease group. AGEs: Advanced glycation end products; NC: Normal control; DKD: Diabetic kidney disease; MSCs: Mesenchymal stem cells.

mitochondria of BMSCs could be transferred to renal PTECs[11] and HUVEC cells[10]. Although recent studies have shown that mitochondrial transfer was bidirectional[31-33], our study did not find that the mitochondria of GECs were transferred to MSCs, which may be due to the difference in the recipient cell species. This finding is consistent with previous investigations[16,34-37] that demonstrated mitochondrial transfer from MSCs to injured target cells.

Mitochondria are energy factories that control cellular survival, stress, and apoptosis[38]. There has been evidence that MSCs can save damaged cells by transferring mitochondria, thus preventing tissue damage and regenerating metabolism[5,10,12]. Co-culturing with MSCs improved ATP production and  $\Delta \Psi_m$  of injured GECs. In addition, our results demonstrated that mitochondria transferred from MSCs

to GECs could reduce apoptosis and promote proliferation in HG-stressed GECs. The finding that mitochondrial transfer reversed target cell proliferation and apoptosis was supported by a previous study conducted by Feng *et al*[10], which showed that MSCs promoted HUVEC proliferation and reduced HUVEC apoptosis through mitochondria transfer from MSCs to injured HUVECs. Additionally, hyperglycemia causes excessive oxidative stress, which contributes significantly to the pathogenesis of diabetic complications[3]. Apoptosis, ROS production, and defective mitophagy play crucial roles in DKD progression[3]. An elevated level of ROS is a biomarker of mitochondrial dysfunction in diabetic kidneys[3]. Fortunately, mitochondrial and intracellular ROS generation was inhibited with MSC supplementation, as well as the variation trend of SOD2 and GPx-3 levels. Furthermore, mitochondrial function was partially improved by MSC-mediated protection in *in vitro* investigations.

Recent studies indicate that mitochondrial dynamics (fusion and fission) play an essential role in mitochondrial distribution, maturation, and quality control[39]. In DKD rats, the fusion and fission of mitochondria are enhanced[4,40], which is similar to our finding that the expression of DRP1 decreased and that of MFN2 increased. Mitochondria play a role in cellular stress-induced apoptosis through various molecular mechanisms. Essentially, mitochondrial toxicity triggers the release of pro-apoptotic factors, which activate latent forms of caspases, resulting in cell death[3]. Importantly, hyperglycemia causes oxidative stress, which initiates caspase activation, leading to the release of TNF- $\alpha$  and activation of the mitochondria-mediated apoptotic pathway[41]. Furthermore, pro-apoptotic factors (caspase 3 and Bax) and inflammation-related factors (IL-6, TNF- $\alpha$ , and IL-1 $\beta$ ) were down-regulated. In contrast, anti-apoptotic factors (Bcl-2) were upregulated after HG-injured GECs were co-cultured with MSCs. Additionally, the ratio of Bcl-2/Bax increased in the HG + MSC group compared to the HG group. However, these differences were minor and did not reach statistical significance. Possible reasons for this might include the following: (1) A too large control (NC and NC + MSC) group could lead to non-statistically significant differences in the HG and HG + MSC groups; and (2) This study had a small sample size, which may result in lower statistical power to detect differences between groups. These reasons may also be applicable to our *in vivo* experimentation and observations. In addition to their importance in intercellular mitochondrial transfer, these factors have also been associated with HG-related damage.

After MSC injection in STZ-induced DKD rats, there was no significant difference in the FBG level compared with the DKD group. This result is in agreement with previous reports[42,43], which may be related to the late treatment of MSCs and the missed opportunity to heal the acute pancreatic injury. Meanwhile, the level of 24 h U-Alb was not significantly different in the DKD + MSC group compared with the DKD group. The reason may be due to the small sample size or the short 2-wk duration of treatment. However, we did identify that the FBG and 24 h U-Alb levels in the DKD + MSC group were lower than those in the DKD group, although there was no statistical significance. Interestingly, a noteworthy finding was that MSCs effectively repaired renal dysfunction (BUN and Scr). Meanwhile, we observed a significant increase in GPx and SOD, indicating that MSCs can protect the kidneys from DKD.

Increased AGEs in DKD is another critical contributing factor resulting in mitochondrial dysfunction and apoptosis of GECs[44]. The main pathological change of DKD is glomerular lesions. A long-term and persistent high-glucose environment can activate protein kinase C and the renin-angiotensin system, induce accumulation of ROS and AGEs that damage endothelial cells, and generate proteinuria and glomerulosclerosis[45], which eventually aggravate renal function damage and progression of DKD. Furthermore, diabetics with glomerular damage may experience altered blood flow and oxygen delivery to other segments of the kidney[3]. However, treatment with MSCs resulted in renal histological changes manifested by reductions in glomerular volume, inflammatory cell infiltration, glomerular basement membrane, and renal interstitial fibrosis, consistent with previously reported results[42]. Therefore, MSCs can improve renal function and pathological changes in DKD to a certain extent.

Potential limitations of our study should be noted. First, further studies are warranted to explore and elucidate the mechanism of mitochondrial transfer from MSCs to injured GECs. For example, Liu *et al*[5] and Han *et al*[13] reported that MSCs transfer mitochondria to injured target cells *via* tunneling nanotubes, and this might be of interest to elucidate the exact mechanism of mitochondrial transfer. In addition, BMSCs can also transfer their mitochondria to target cells *via* gap junction channels containing the connexin 43 protein[12], extracellular vesicles[46], or endocytosis[47]. Second, since the laboratory conditions were unable to freeze renal tissue when they were obtained, the distribution of MSC mitochondria labeled with fluorescence in the tissue was not observed. Future studies are recommended to observe the map of MSC-derived mitochondria in DKD kidney tissue. Third, whether mitochondrial transfer from MSCs to GECs directly affects the function of GEC needs further verification by blocking the mitochondrial transfer. Fourth, TUNEL detects the apoptosis of cells in the whole kidney tissue, but it could not distinguish the apoptosis of GECs. Therefore, multiple fluorescent markers may be used for added analyses. Fifth, we did not assess the percentage of GECs with transferred MSC mitochondria. Our current objective focused on how to promote mitochondrial transfer from BMSC to GECs. Sixth, a study has shown that with intravenous injection of MSCs, these cells do not reach the damage site but release exosomes that can[48]. The article also reported that neither infusion of MSCs induced

significant fibrotic responses in organs (lungs, kidney, liver, and spleen), which might cause safety concerns. In our study, we did not assess the following issues: (1) The dynamic changes in the biodistribution of the BMSCs and the ratio/number of BMSCs after the injection; (2) The safety of the BMSC injection; and (3) The level of liver injury (aspartate aminotransferase, alanine aminotransferase, and others). However, we are optimistic about being able to solve these problems in our ongoing research.

## CONCLUSION

Our study provides insights into the mechanisms underlying MSCs' ability to rescue injured GECs by a new cell-to-cell communication method of mitochondria transfer. Notably, mitochondria transfer alleviates mitochondrial damage and abates cellular apoptosis of GECs. Furthermore, the therapeutic effects of BMSC on DKD rats may be related to this mechanism of mitochondrial transfer.

## ARTICLE HIGHLIGHTS

### Research background

Mesenchymal stem cells (MSCs) can rescue injured target cells *via* mitochondrial transfer. However, little is known about how bone marrow-derived MSCs repair glomeruli in diabetic kidney disease (DKD).

### Research motivation

Mitochondria play vital roles in biological processes such as oxidative phosphorylation, cellular metabolism, and cell death. Recent studies indicate that mitochondrial damage occurs in glomerular endothelial cells (GECs) in DKD and MSCs could transfer their mitochondria to target cells. However, the mechanism of how mitochondrial transfer contributes to the high glucose-injured GECs is not well-understood.

### Research objectives

To investigate the mechanisms of mitochondrial transfer between MSC and high glucose-injured GECs or streptozotocin (STZ)-induced DKD rats.

### Research methods

The mitochondria of GECs and MSCs were labeled before co-cultivation. A fluorescence microscope was used to examine the mitochondrial transfer, then cell proliferation and apoptosis were detected by western blot, real-time reverse transcriptase-polymerase chain reaction, Cell Counting Kit-8, and Annexin V-FITC/PI assays. The mitochondria function [adenosine triphosphate (ATP), reactive oxygen species (ROS), and mitochondrial membrane potential] of GECs was assessed with related-detection kits. A DKD rat model was obtained by STZ administration. Renal function and oxidative stress were detected with an automatic biochemical analyzer and related-detection kits. In addition, histological changes were evaluated by hematoxylin and eosin, periodic acid-Schiff, and immunohistochemical staining.

### Research results

Our results demonstrated that the MitoTracker Red CMXRos labeled mitochondria were transferred from MSCs to the high glucose-injured GECs, ATP levels were increased, and the membrane potential of mitochondria was stabilized. Additionally, the transfer of mitochondria decreased pro-inflammatory cytokines [interleukin (IL)-6, IL-1 $\beta$ , and tumor necrosis factor- $\alpha$ ] and pro-apoptotic factors (caspase 3 and Bax). Transfer of healthy MSC-derived mitochondria enhanced the expression of superoxide dismutase 2, B-cell lymphoma 2, glutathione peroxidase 3, and Mitofusin 2 and inhibited ROS (mitochondrial and intracellular) and dynamin-related protein 1 expression. Notably, a transfer of healthy mitochondria from MSCs suppressed GEC apoptosis and enhanced their proliferation. Furthermore, STZ-induced DKD animal experiments showed that MSC ameliorated renal function damage and pathological progression of DKD.

### Research conclusions

Our data demonstrated the existing of mitochondrial transfer *in vitro*, which plays a pivotal role in the rescue of GECs. Moreover, MSCs repair the renal function damage and pathological progress of DKD rats perhaps *via* mechanism of mitochondrial transfer.

### Research perspectives

This study revealed the role and mechanism of mitochondrial transfer in the rescue of injured GECs,

which can provide a scientific basis for the potential therapeutic effects of MSCs on DKD.

## ACKNOWLEDGEMENTS

We express our sincere gratitude to our institution for its support and funding. Furthermore, all authors are grateful for the School of Medicine of Southeast University and its experimental platform.

## FOOTNOTES

**Author contributions:** Tang LX, Wei B, Li K, and Xu H designed the study; Tang LX and Wei B wrote the manuscript; Tang LX, Wei B, Jiang LY, Ying YY, Chen TX, Huang RF, and Shi MJ performed the experiments; Tang LX, Wei B, Li K, and Xu H analysed the data; and all authors have read and approved the final manuscript.

**Supported by** the Science and Technology Foundation of Jinhua, No. 2021-4-190.

**Institutional animal care and use committee statement:** The animal experiments were carried out following the National Institutes of Health Guidelines for the care and use of laboratory animals and according to protocols approved by the Animal Experimental Ethical Committee of Southeast University (Nanjing, China). The animals were acclimatized to laboratory conditions (22-25 °C, 12 h/12 h light/dark, 50% humidity, *ad libitum* access to food and water). All animals were euthanized by 2%-3% halothane and then carbon dioxide inhalation for kidney tissue collection.

**Conflict-of-interest statement:** All the authors report no relevant conflicts of interest for this article.

**Data sharing statement:** The datasets supporting the conclusions of this article are included within the article.

**ARRIVE guidelines statement:** The authors have read the ARRIVE guidelines, and the manuscript was prepared and revised according to the ARRIVE guidelines.

**Open-Access:** This article is an open-access article that was selected by an in-house editor and fully peer-reviewed by external reviewers. It is distributed in accordance with the Creative Commons Attribution NonCommercial (CC BY-NC 4.0) license, which permits others to distribute, remix, adapt, build upon this work non-commercially, and license their derivative works on different terms, provided the original work is properly cited and the use is non-commercial. See: <https://creativecommons.org/licenses/by-nc/4.0/>

**Country/Territory of origin:** China

**ORCID number:** Li-Xia Tang 0000-0002-5429-9146; Bing Wei 0000-0002-3398-8364; Lu-Yao Jiang 0000-0002-7745-2676; You-You Ying 0000-0001-5502-9087; Ke Li 0000-0002-4762-7711; Tian-Xi Chen 0000-0003-2112-3600; Ruo-Fei Huang 0000-0002-3032-7886; Miao-Jun Shi 0000-0001-9772-9268; Hang Xu 0000-0001-6304-5693.

**S-Editor:** Wang JJ

**L-Editor:** Wang TQ

**P-Editor:** Guo X

## REFERENCES

- 1 **GBD Chronic Kidney Disease Collaboration.** Global, regional, and national burden of chronic kidney disease, 1990-2017: a systematic analysis for the Global Burden of Disease Study 2017. *Lancet* 2020; **395**: 709-733 [PMID: 32061315 DOI: 10.1016/S0140-6736(20)30045-3]
- 2 **Yoshioka K,** Hirakawa Y, Kurano M, Ube Y, Ono Y, Kojima K, Iwama T, Kano K, Hasegawa S, Inoue T, Shimada T, Aoki J, Yatomi Y, Nangaku M, Inagi R. Lysophosphatidylcholine mediates fast decline in kidney function in diabetic kidney disease. *Kidney Int* 2022; **101**: 510-526 [PMID: 34856312 DOI: 10.1016/j.kint.2021.10.039]
- 3 **Wei PZ,** Szeto CC. Mitochondrial dysfunction in diabetic kidney disease. *Clin Chim Acta* 2019; **496**: 108-116 [PMID: 31276635 DOI: 10.1016/j.cca.2019.07.005]
- 4 **Forbes JM,** Thorburn DR. Mitochondrial dysfunction in diabetic kidney disease. *Nat Rev Nephrol* 2018; **14**: 291-312 [PMID: 29456246 DOI: 10.1038/nrneph.2018.9]
- 5 **Liu K,** Ji K, Guo L, Wu W, Lu H, Shan P, Yan C. Mesenchymal stem cells rescue injured endothelial cells in an *in vitro* ischemia-reperfusion model via tunneling nanotube like structure-mediated mitochondrial transfer. *Microvasc Res* 2014; **92**: 10-18 [PMID: 24486322 DOI: 10.1016/j.mvr.2014.01.008]
- 6 **Qi H,** Casalena G, Shi S, Yu L, Ebefors K, Sun Y, Zhang W, D'Agati V, Schlondorff D, Haraldsson B, Böttinger E, Daehn I. Glomerular Endothelial Mitochondrial Dysfunction Is Essential and Characteristic of Diabetic Kidney Disease

- Susceptibility. *Diabetes* 2017; **66**: 763-778 [PMID: 27899487 DOI: 10.2337/db16-0695]
- 7 **Qi W**, Keenan HA, Li Q, Ishikado A, Kannt A, Sadowski T, Yorek MA, Wu IH, Lockhart S, Coppely LJ, Pfenninger A, Liew CW, Qiang G, Burkart AM, Hastings S, Pober D, Cahill C, Niewczas MA, Israelsen WJ, Tinsley L, Stillman IE, Amenta PS, Feener EP, Vander Heiden MG, Stanton RC, King GL. Pyruvate kinase M2 activation may protect against the progression of diabetic glomerular pathology and mitochondrial dysfunction. *Nat Med* 2017; **23**: 753-762 [PMID: 28436957 DOI: 10.1038/nm.4328]
  - 8 **Reidy K**, Kang HM, Hostetter T, Susztak K. Molecular mechanisms of diabetic kidney disease. *J Clin Invest* 2014; **124**: 2333-2340 [PMID: 24892707 DOI: 10.1172/JCI12271]
  - 9 **Hayakawa K**, Chan SJ, Mandeville ET, Park JH, Bruzzese M, Montaner J, Arai K, Rosell A, Lo EH. Protective Effects of Endothelial Progenitor Cell-Derived Extracellular Mitochondria in Brain Endothelium. *Stem Cells* 2018; **36**: 1404-1410 [PMID: 29781122 DOI: 10.1002/stem.2856]
  - 10 **Feng Y**, Zhu R, Shen J, Wu J, Lu W, Zhang J, Liu K. Human Bone Marrow Mesenchymal Stem Cells Rescue Endothelial Cells Experiencing Chemotherapy Stress by Mitochondrial Transfer Via Tunneling Nanotubes. *Stem Cells Dev* 2019; **28**: 674-682 [PMID: 30808254 DOI: 10.1089/scd.2018.0248]
  - 11 **Konari N**, Nagaishi K, Kikuchi S, Fujimiya M. Mitochondria transfer from mesenchymal stem cells structurally and functionally repairs renal proximal tubular epithelial cells in diabetic nephropathy in vivo. *Sci Rep* 2019; **9**: 5184 [PMID: 30914727 DOI: 10.1038/s41598-019-40163-y]
  - 12 **Islam MN**, Das SR, Emin MT, Wei M, Sun L, Westphalen K, Rowlands DJ, Quadri SK, Bhattacharya S, Bhattacharya J. Mitochondrial transfer from bone-marrow-derived stromal cells to pulmonary alveoli protects against acute lung injury. *Nat Med* 2012; **18**: 759-765 [PMID: 22504485 DOI: 10.1038/nm.2736]
  - 13 **Han H**, Hu J, Yan Q, Zhu J, Zhu Z, Chen Y, Sun J, Zhang R. Bone marrow-derived mesenchymal stem cells rescue injured H9c2 cells via transferring intact mitochondria through tunneling nanotubes in an *in vitro* simulated ischemia/reperfusion model. *Mol Med Rep* 2016; **13**: 1517-1524 [PMID: 26718099 DOI: 10.3892/mmr.2015.4726]
  - 14 **Zhang J**, Zhang J, Zhao L, Xin Y, Liu S, Cui W. Differential roles of microtubules in the two formation stages of membrane nanotubes between human mesenchymal stem cells and neonatal mouse cardiomyocytes. *Biochem Biophys Res Commun* 2019; **512**: 441-447 [PMID: 30904163 DOI: 10.1016/j.bbrc.2019.03.075]
  - 15 **Fergie N**, Todd N, McClements L, McAuley D, O'Kane C, Krasnodembskaya A. Hypercapnic acidosis induces mitochondrial dysfunction and impairs the ability of mesenchymal stem cells to promote distal lung epithelial repair. *FASEB J* 2019; **33**: 5585-5598 [PMID: 30649987 DOI: 10.1096/fj.201802056R]
  - 16 **Babenko VA**, Silachev DN, Popkov VA, Zorova LD, Pevzner IB, Plotnikov EY, Sukhikh GT, Zorov DB. Miro1 Enhances Mitochondria Transfer from Multipotent Mesenchymal Stem Cells (MMSC) to Neural Cells and Improves the Efficacy of Cell Recovery. *Molecules* 2018; **23** [PMID: 29562677 DOI: 10.3390/molecules23030687]
  - 17 **Shanmughapriya S**, Langford D, Natarajaseenivasan K. Inter and Intracellular mitochondrial trafficking in health and disease. *Ageing Res Rev* 2020; **62**: 101128 [PMID: 32712108 DOI: 10.1016/j.arr.2020.101128]
  - 18 **Galvan DL**, Long J, Green N, Chang BH, Lin JS, Schumacker P, Truong LD, Overbeek P, Danesh FR. Drp1S600 phosphorylation regulates mitochondrial fission and progression of nephropathy in diabetic mice. *J Clin Invest* 2019; **129**: 2807-2823 [PMID: 31063459 DOI: 10.1172/JCI127277]
  - 19 **Gong L**, Chen B, Zhang J, Sun Y, Yuan J, Niu X, Hu G, Chen Y, Xie Z, Deng Z, Li Q, Wang Y. Human ESC-sEVs alleviate age-related bone loss by rejuvenating senescent bone marrow-derived mesenchymal stem cells. *J Extracell Vesicles* 2020; **9**: 1800971 [PMID: 32944188 DOI: 10.1080/20013078.2020.1800971]
  - 20 **Livingston MJ**, Wang J, Zhou J, Wu G, Ganley IG, Hill JA, Yin XM, Dong Z. Clearance of damaged mitochondria via mitophagy is important to the protective effect of ischemic preconditioning in kidneys. *Autophagy* 2019; **15**: 2142-2162 [PMID: 31066324 DOI: 10.1080/15548627.2019.1615822]
  - 21 **Li B**, Zheng Z, Wei Y, Wang M, Peng J, Kang T, Huang X, Xiao J, Li Y, Li Z. Therapeutic effects of neuregulin-1 in diabetic cardiomyopathy rats. *Cardiovasc Diabetol* 2011; **10**: 69 [PMID: 21798071 DOI: 10.1186/1475-2840-10-69]
  - 22 **Bhakkialakshmi E**, Shalini D, Sekar TV, Rajaguru P, Paulmurugan R, Ramkumar KM. Therapeutic potential of pterostilbene against pancreatic beta-cell apoptosis mediated through Nrf2. *Br J Pharmacol* 2014; **171**: 1747-1757 [PMID: 24417315 DOI: 10.1111/bph.12577]
  - 23 **Choi HJ**, Choi S, Kim JG, Song MH, Shim KS, Lim YM, Kim HJ, Park K, Kim SE. Enhanced tendon restoration effects of anti-inflammatory, lactoferrin-immobilized, heparin-polymeric nanoparticles in an Achilles tendinitis rat model. *Carbohydr Polym* 2020; **241**: 116284 [PMID: 32507170 DOI: 10.1016/j.carbpol.2020.116284]
  - 24 **Wu PT**, Su WR, Li CL, Hsieh JL, Ma CH, Wu CL, Kuo LC, Jou IM, Chen SY. Inhibition of CD44 induces apoptosis, inflammation, and matrix metalloproteinase expression in tendinopathy. *J Biol Chem* 2019; **294**: 20177-20184 [PMID: 31732563 DOI: 10.1074/jbc.RA119.009675]
  - 25 **Tang L**, Li K, Zhang Y, Li H, Li A, Xu Y, Wei B. Quercetin liposomes ameliorate streptozotocin-induced diabetic nephropathy in diabetic rats. *Sci Rep* 2020; **10**: 2440 [PMID: 32051470 DOI: 10.1038/s41598-020-59411-7]
  - 26 **Yue T**, Xu HL, Chen PP, Zheng L, Huang Q, Sheng WS, Zhuang YD, Jiao LZ, Chi TT, ZhuGe DL, Liu JJ, Zhao YZ, Lan L. Combination of coenzyme Q10-loaded liposomes with ultrasound targeted microbubbles destruction (UTMD) for early theranostics of diabetic nephropathy. *Int J Pharm* 2017; **528**: 664-674 [PMID: 28642201 DOI: 10.1016/j.ijpharm.2017.06.070]
  - 27 **Shiogama K**, Kitazawa K, Mizutani Y, Onouchi T, Inada K, Tsutsumi Y. New Grocott Stain without Using Chromic Acid. *Acta Histochem Cytochem* 2015; **48**: 9-14 [PMID: 25861133 DOI: 10.1267/ahc.14045]
  - 28 **Kunter U**, Rong S, Djuric Z, Boor P, Müller-Newen G, Yu D, Floege J. Transplanted mesenchymal stem cells accelerate glomerular healing in experimental glomerulonephritis. *J Am Soc Nephrol* 2006; **17**: 2202-2212 [PMID: 16790513 DOI: 10.1681/ASN.2005080815]
  - 29 **Almeida A**, Lira R, Oliveira M, Martins M, Azevedo Y, Silva KR, Carvalho S, Cortez E, Stumbo AC, Carvalho L, Thole A. Bone marrow-derived mesenchymal stem cells transplantation ameliorates renal injury through anti-fibrotic and anti-inflammatory effects in chronic experimental renovascular disease. *Biomed J* 2022; **45**: 629-641 [PMID: 34333108 DOI: 10.1016/j.bj.2021.07.009]

- 30 **Boukelmoune N**, Chiu GS, Kavelaars A, Heijnen CJ. Mitochondrial transfer from mesenchymal stem cells to neural stem cells protects against the neurotoxic effects of cisplatin. *Acta Neuropathol Commun* 2018; **6**: 139 [PMID: 30541620 DOI: 10.1186/s40478-018-0644-8]
- 31 **Mahrouf-Yorgov M**, Augeul L, Da Silva CC, Jourdan M, Rigolet M, Manin S, Ferrera R, Ovize M, Henry A, Guguin A, Meningaud JP, Dubois-Randé JL, Motterlini R, Foresti R, Rodriguez AM. Mesenchymal stem cells sense mitochondria released from damaged cells as danger signals to activate their rescue properties. *Cell Death Differ* 2017; **24**: 1224-1238 [PMID: 28524859 DOI: 10.1038/cdd.2017.51]
- 32 **Zhang Y**, Yu Z, Jiang D, Liang X, Liao S, Zhang Z, Yue W, Li X, Chiu SM, Chai YH, Liang Y, Chow Y, Han S, Xu A, Tse HF, Lian Q. iPSC-MSCs with High Intrinsic MIRO1 and Sensitivity to TNF- $\alpha$  Yield Efficacious Mitochondrial Transfer to Rescue Anthracycline-Induced Cardiomyopathy. *Stem Cell Reports* 2016; **7**: 749-763 [PMID: 27641650 DOI: 10.1016/j.stemcr.2016.08.009]
- 33 **Melcher M**, Danhauser K, Seibt A, Degistirici Ö, Baertling F, Kondadi AK, Reichert AS, Koopman WJH, Willems PHGM, Rodenburg RJ, Mayatepek E, Meisel R, Distelmaier F. Modulation of oxidative phosphorylation and redox homeostasis in mitochondrial NDUFS4 deficiency via mesenchymal stem cells. *Stem Cell Res Ther* 2017; **8**: 150 [PMID: 28646906 DOI: 10.1186/s13287-017-0601-7]
- 34 **Yang H**, Borg TK, Ma Z, Xu M, Wetzel G, Saraf LV, Markwald R, Runyan RB, Gao BZ. Biochip-based study of unidirectional mitochondrial transfer from stem cells to myocytes via tunneling nanotubes. *Biofabrication* 2016; **8**: 015012 [PMID: 26844857 DOI: 10.1088/1758-5090/8/1/015012]
- 35 **Court AC**, Le-Gatt A, Luz-Crawford P, Parra E, Aliaga-Tobar V, Bátiz LF, Contreras RA, Ortúzar MI, Kurte M, Elizondo-Vega R, Maracaja-Coutinho V, Pino-Lagos K, Figueroa FE, Khoury M. Mitochondrial transfer from MSCs to T cells induces Treg differentiation and restricts inflammatory response. *EMBO Rep* 2020; **21**: e48052 [PMID: 31984629 DOI: 10.15252/embr.201948052]
- 36 **Yang Y**, Ye G, Zhang YL, He HW, Yu BQ, Hong YM, You W, Li X. Transfer of mitochondria from mesenchymal stem cells derived from induced pluripotent stem cells attenuates hypoxia-ischemia-induced mitochondrial dysfunction in PC12 cells. *Neural Regen Res* 2020; **15**: 464-472 [PMID: 31571658 DOI: 10.4103/1673-5374.266058]
- 37 **Jiang D**, Xiong G, Feng H, Zhang Z, Chen P, Yan B, Chen L, Gandhervin K, Ma C, Li C, Han S, Zhang Y, Liao C, Lee TL, Tse HF, Fu QL, Chiu K, Lian Q. Donation of mitochondria by iPSC-derived mesenchymal stem cells protects retinal ganglion cells against mitochondrial complex I defect-induced degeneration. *Theranostics* 2019; **9**: 2395-2410 [PMID: 31149051 DOI: 10.7150/thno.29422]
- 38 **Sinclair KA**, Yerkovich ST, Hopkins PM, Chambers DC. Characterization of intercellular communication and mitochondrial donation by mesenchymal stromal cells derived from the human lung. *Stem Cell Res Ther* 2016; **7**: 91 [PMID: 27406134 DOI: 10.1186/s13287-016-0354-8]
- 39 **Martin OJ**, Lai L, Soundarapandian MM, Leone TC, Zorzano A, Keller MP, Attie AD, Muoio DM, Kelly DP. A role for peroxisome proliferator-activated receptor  $\gamma$  coactivator-1 in the control of mitochondrial dynamics during postnatal cardiac growth. *Circ Res* 2014; **114**: 626-636 [PMID: 24366168 DOI: 10.1161/CIRCRESAHA.114.302562]
- 40 **Bhargava P**, Schnellmann RG. Mitochondrial energetics in the kidney. *Nat Rev Nephrol* 2017; **13**: 629-646 [PMID: 28804120 DOI: 10.1038/nrneph.2017.107]
- 41 **Pal PB**, Sinha K, Sil PC. Mangiferin attenuates diabetic nephropathy by inhibiting oxidative stress mediated signaling cascade, TNF $\alpha$  related and mitochondrial dependent apoptotic pathways in streptozotocin-induced diabetic rats. *PLoS One* 2014; **9**: e107220 [PMID: 25233093 DOI: 10.1371/journal.pone.0107220]
- 42 **Xiang E**, Han B, Zhang Q, Rao W, Wang Z, Chang C, Zhang Y, Tu C, Li C, Wu D. Human umbilical cord-derived mesenchymal stem cells prevent the progression of early diabetic nephropathy through inhibiting inflammation and fibrosis. *Stem Cell Res Ther* 2020; **11**: 336 [PMID: 32746936 DOI: 10.1186/s13287-020-01852-y]
- 43 **Ezquer F**, Ezquer M, Simon V, Pardo F, Yañez A, Carpio D, Conget P. Endovenous administration of bone-marrow-derived multipotent mesenchymal stromal cells prevents renal failure in diabetic mice. *Biol Blood Marrow Transplant* 2009; **15**: 1354-1365 [PMID: 19822294 DOI: 10.1016/j.bbmt.2009.07.022]
- 44 **Zhang B**, Zhang X, Zhang C, Shen Q, Sun G, Sun X. Notoginsenoside R1 Protects db/db Mice against Diabetic Nephropathy via Upregulation of Nrf2-Mediated HO-1 Expression. *Molecules* 2019; **24** [PMID: 30634720 DOI: 10.3390/molecules24020247]
- 45 **Jourde-Chiche N**, Fakhouri F, Dou L, Bellien J, Burtey S, Frimat M, Jarrot PA, Kaplanski G, Le Quintrec M, Pernin V, Rigother C, Sallée M, Fremeaux-Bacchi V, Guerrot D, Roumenina LT. Endothelium structure and function in kidney health and disease. *Nat Rev Nephrol* 2019; **15**: 87-108 [PMID: 30607032 DOI: 10.1038/s41581-018-0098-z]
- 46 **Tkach M**, Théry C. Communication by Extracellular Vesicles: Where We Are and Where We Need to Go. *Cell* 2016; **164**: 1226-1232 [PMID: 26967288 DOI: 10.1016/j.cell.2016.01.043]
- 47 **Sun C**, Liu X, Wang B, Wang Z, Liu Y, Di C, Si J, Li H, Wu Q, Xu D, Li J, Li G, Wang Y, Wang F, Zhang H. Endocytosis-mediated mitochondrial transplantation: Transferring normal human astrocytic mitochondria into glioma cells rescues aerobic respiration and enhances radiosensitivity. *Theranostics* 2019; **9**: 3595-3607 [PMID: 31281500 DOI: 10.7150/thno.33100]
- 48 **Nakazaki M**, Morita T, Lankford KL, Askenase PW, Kocsis JD. Small extracellular vesicles released by infused mesenchymal stromal cells target M2 macrophages and promote TGF- $\beta$  upregulation, microvascular stabilization and functional recovery in a rodent model of severe spinal cord injury. *J Extracell Vesicles* 2021; **10**: e12137 [PMID: 34478241 DOI: 10.1002/jev2.12137]



Published by **Baishideng Publishing Group Inc**  
7041 Koll Center Parkway, Suite 160, Pleasanton, CA 94566, USA  
**Telephone:** +1-925-3991568  
**E-mail:** [bpgoffice@wjgnet.com](mailto:bpgoffice@wjgnet.com)  
**Help Desk:** <https://www.f6publishing.com/helpdesk>  
<https://www.wjgnet.com>

